Iranian Journal of Operations Research
Vol. 3, No. 1, 2012, pp. 46-60

T-lymphocyte Cell Injection Cancer Immunotherapy: an Optimal Control Approach

H. Basirzadeh[1,*], S. Nazari[2]

We consider a mathematical model in the form of a system of ordinary differential equations (ODE) for optimally administrating cancer treatments. The ODE system dynamics characterized by locating equilibrium points and stability properties are determined by linearization and using appropriate Lyapunov functions. By applying optimal control theory, we seek to minimize the cost function associated with the vaccine therapy looking for minimization of the tumor cells. Global existence of a solution is shown for this model and existence of an optimal control is proven. The optimality conditions and characterization of the control are discussed.

***Keywords*:** *Tumor, Vaccine therapy, Tumor infiltrating lymphocyte, Quadratic optimal controls, Lyapunov function.*

Manuscript received on 5/07/2011 and accepted for publication on 12/12/2011.

1. Introduction

Mathematical modeling of tumor growth and immunotherapy has been approached by a number of researchers using a variety of models over the past decades [1, 2, 3, 10, 12, 15, 17].

Anew mathematical model of tumor-immune interactions sheds light on the differing roles of the natural killer (NK) and $CD8^+$ T cells in suppressing various tumor cell lines in mice and humans [7].

Antibacterial and antiviral vaccines are used for prophylaxis. They are effective in preventing the occurrence of disease when the host encounters the targeted pathogenic microorganism. Cancer vaccines open an exciting new world for cancer therapy. They are used with a therapeutic intent. The goal is to stimulate the patient's immune system to produce specific immune-effector cells and antibodies targeting preexisting tumor cells to lead to their elimination. Despite decades of studies and notable successes in murine models, no cancer vaccine has yet achieved approval for use in human cancers. Advances in immunology such as the discovery of how the immune system recognizes antigens and how immune responses are regulated have generated renewed interest in this field. Malignant melanoma has been the tumor most often targeted by vaccines, partly because of the ready availability of tumor cells and the ease of growth of cells in the laboratory [16]. A few selected clinical trials will serve as examples [4, 13].

2. Background

2.1. Biological Aspects

*Corresponding Author.
[1]Department of Mathematical and Computer Sciences, Shahid Chamran University, P.O. Box 83151-61357, Ahvaz, Iran
E-mail: basirzad@scu.ac.ir.
[2]Department of Mathematical and Computer Sciences, Shahid Chamran University, P.O. Box 83151-61357, Ahvaz, Iran
E-mail: Sanaz.Nazari@gmail.com.

NK cells are large granular lymphocytes that do not express markers of either T- or B-cell lineage. As a constituent of innate immunity, they recognize and destroy tumor cells, among others, independent of prior exposure. NK cells are thought to play an important role in preventing the development of clinical cancer by killing abnormal cells before they multiply and grow.

T cells, which carry the $CD3^+$ marker, are morphologically small lymphocytes in the peripheral blood. They develop in the thymus and orchestrate the immune system response to infected or malignant cells. $CD3^+CD8^+$ T cells (also called $CD8^+$ T cells) are a critical subpopulation of T-lymphocytes which can be cytotoxic to tumor cells that a provided that a previous sensitization has occurred [6].

2.2. The Model Overview

The mathematical structure of the model is built on an earlier modeling work of Pillis [7] in which the tumor growth, an innate and specific immune response, is represented by a system of differential equations. The cell populations in this model at time *t* are denoted by:

- $T(t)$, tumor cell population at time *t.*
- $N(t)$, total level of NK cell effectiveness at time *t.*
- $L(t)$, total level of tumor-specific $CD8^+$ T-cell effectiveness at time *t.*

The system of differential equations (Eq. 1-3) describing the growth, death, and interactions of these populations is given by

$$\frac{dT}{dt} = aT(1 - bT) - cNT - D \tag{1}$$

$$\frac{dN}{dt} = \sigma - fN + \frac{gT^2}{h+T^2}N - pNT \tag{2}$$

$$\frac{dL}{dt} = -mL + \frac{jD^2}{k+D^2}L - qLT + rNT \tag{3}$$

$$D = d\frac{(L/T)^\lambda}{s+(L/T)^\lambda}T. \tag{4}$$

These equations have the general initial conditions $T(0) = T_0$, $N(0) = N_0$ and $L(0) = L_0$, where each initial value is positive. In Eq. (1), the tumor cell population is assumed to grow logistically, while tumor cells are killed by both the NK cells and $CD8^+$ T cells. Pillis introduced a new functional form for the ($CD8^+$ T)-tumor kills term, represented by D in Eq. (2), given explicitly by Eq. (4). In Eq. (2), the NK cells have a constant source rate σ, while death is proportional to the population of NK cells through the term $-fN$. The NK cells are also recruited by tumor cells through a Michaelis–Menten term, $\frac{gT^2}{h+T^2}$, serving to provide a saturation effect. Additionally, NK cells are inactivated through contact with tumor cells according to a mass-action dynamic. In the case of the $CD8^+$ T cells, in addition to being recruited by interactions with T-cell processed tumor cells through a Michaelis-Menten dynamic, additional $CD8^+$ T cells are stimulated by the interaction of NK cells with tumor cells. This NK stimulation is represented by the *rNT* term in Eq. (3). For all the experiments, model parameters are set to the values given in Table 1.

Table 1. Estimated patient-specific human variables [7]

Parameters	Units	Estimated value	Description
a	Day^{-1}	5.14×10^{-1}	Tumor growth rate
b	$cell^{-1}$	1.02×10^{-9}	1/b is tumor carrying capacity
c	$cell^{-1}\ day^{-1}$	3.23×10^{-7}	Fractional tumor cell kill by NK cells
d	day^{-1}	5.80	Saturation level of fractional tumor cell kill by CD8+ T cells
λ	None	1.36	Exponent of fractional tumor cell kill by CD8+ T cells
s	None	2.5×10^{-1}	Steepness coefficient of the tumor-(CD8+ T cell) competition term
σ	$cells\ day^{-1}$	1.3×10^{4}	Constant source of NK cells
f	day^{-1}	4.12×10^{-2}	Death rate of NK cells
g	day^{-1}	2.5×10^{-2}	Maximum NK cell recruitment rate by tumor cells
h	$cell^{2}$	2.02×10^{7}	Steepness coefficient of the NK cell recruitment curve
p	$cell^{-1}\ day^{-1}$	1.00×10^{-7}	NK cell inactivation rate by tumor cells
m	day^{-1}	2.00×10^{-2}	Death rate of CD8+ T cells
j	day^{-1}	3.75×10^{-2}	Maximum CD8+ T-cell recruitment rate
k	$cell^{2}$	2.0×10^{7}	Steepness coefficient of the CD8+ T-cell recruitment curve
q	$cell^{-1}\ day^{-1}$	3.42×10^{-10}	CD8+ T-cell inactivation rate by tumor cells
r	$cell^{-1}\ day^{-1}$	1.1×10^{-7}	Rate at which tumor-specific CD8+ T cells are stimulated to be produced as a result of tumor cells killed by NK cells

3. Dynamics

3.1. Determination of Equilibrium Points and their Stability

Theorem 1. Suppose that J is an $n \times n$ matrix of real constants. Furthermore, suppose $\vec{P}(\vec{x})$ is a vector-valued function that is continuously differentiable in an open ball $B_r(\vec{p})$, that $\vec{P}(\vec{p}) = 0$, and that $\vec{P}(\vec{x})$ has an order at least 2 at $\vec{p}$. Then the nearly linear system:

$$\frac{d\vec{x}}{dt} = J(\vec{x} - \vec{p}) + \vec{P}(\vec{x})$$

has the following properties:

(1) The system is asymptotically stable at $\vec{p}$ if all the eigenvalues of J have negative real parts.

(2) The system is unstable at $\vec{p}$ if there is at least one eigenvalue of J with positive real part.

In order to study the equilibrium points of the system and its stability, we set the three equations (1)-(3) simultaneously equal to zero in order to find the equilibrium.

For the case $T_E \neq 0$, the values of equilibrium points for a non-zero tumor must be found numerically [6].

In particular, setting (2) to zero and solving for *N*, yields

$$N_E = \frac{\sigma(h + T^2)}{fh + (f - g)T^2 + phT + pT^3}.$$

Similarly, by requiring (1) to equal zero, we have

$$\bar{D}_E = a - abT - cN_E,$$

$$\text{with } D = \bar{D}T.$$

Using the last expression in (4) gives an expression for L:

$$L_{\mathrm{E1}} = \left(\frac{\bar{D}_E \mathrm{s} T^{\lambda}}{(\mathrm{d} - \bar{D}_E)}\right)^{1/\lambda}. \quad (5)$$

Finally, setting equation (3) to zero gives

$$L_{\mathrm{E2}} = rN_E T/\left(m - \frac{j\bar{D}_E{}^2 T^2}{k + \bar{D}_E{}^2 T^2} + qT.\right) \quad (6)$$

Equilibrium points of the system (1)-(3) are found by intersecting (5) and (6). The solutions are graphed in Fig. 1.

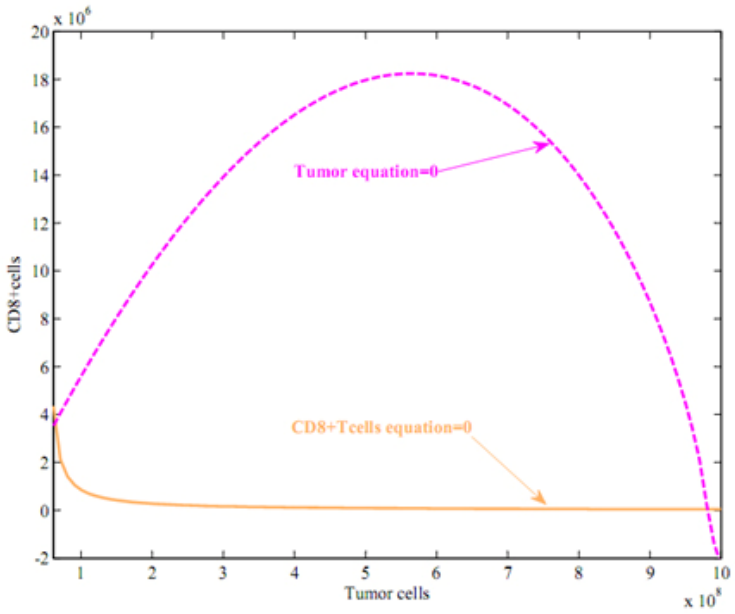

Figure 1. Non-zero equilibrium points of functions

Fig. 2 gives simulations of the phase portraits of these systems. There are two equilibrium points predicted by the model as denoted by *A* and *B*. For illustrative purposes, Fig. 2 shows the state

trajectories predicted by the model for different initial conditions in the simplest case in which the model has only two state variables ($n = 2$).

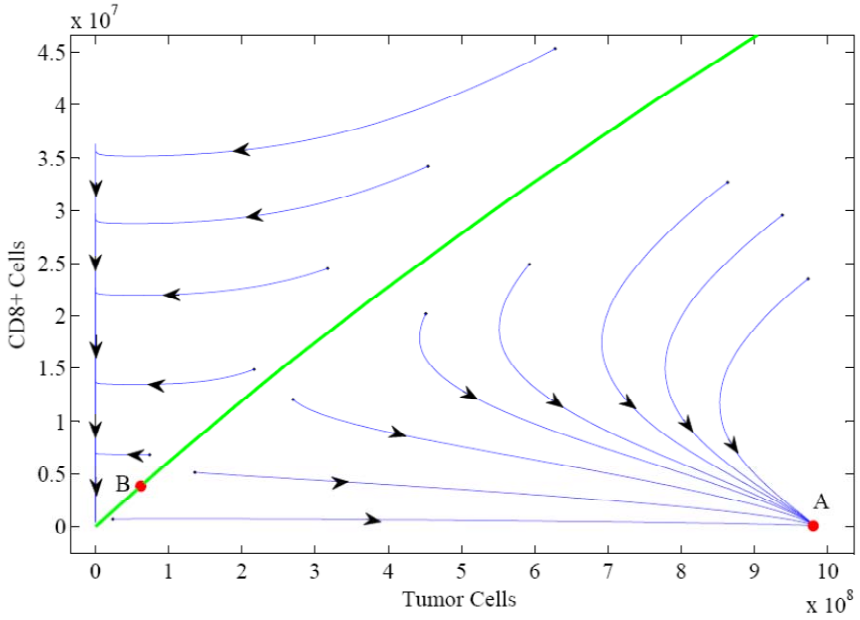

Figure 2. Simulations of the phase portraits of systems

Stability of the equilibrium is determined by linearization of the system about the calculated values, and by determining the stability of the linearized system (Fig. 3(a) and Fig. 3(b). The stability of tumor free points is important from a physiological viewpoint. If the system is in a healthy state, but the point is unstable, a small perturbation from the a healthy state will cause the system to move away from the point and evolve toward the stable equilibrium ($T_E \neq 0$).

The equilibrium point labeled *A* (Fig. 3(a)) is a stable node (nodal sink), characterized by a relatively high tumor burden (9.80×10^8 cells) and a relatively low $CD8^+$ cells (4.48×10^4cells) level, corresponds to a relatively "uncontrolled" tumor growth or "tumor escape". The eigenvalues of the Jacobian corresponding to the point *A* are:

$$e_1 = -0.5033, \qquad e_2 = -0.8646, \qquad e_3 = -0.3162.$$

Thus, the $T = 9.80\times10^8$ equilibrium point is locally asymptotically stable.

Also, the equilibrium point labeled as *B* (Fig. (3b)) is an unstable saddle point, characterized by a relatively low tumor burden (6.2×10^7 cells) and a relatively high $CD8^+$ cells (3.8×10^6cells). The eigenvalues of the Jacobian for the point *B* are:

$$e_1 = 0.5737, \qquad e_2 = -9.723, \qquad e_3 = -0.0034.$$

Thus, the $T = 6.80\times10^7$ equilibrium point is unstable, because $e_1 \geq 0$.

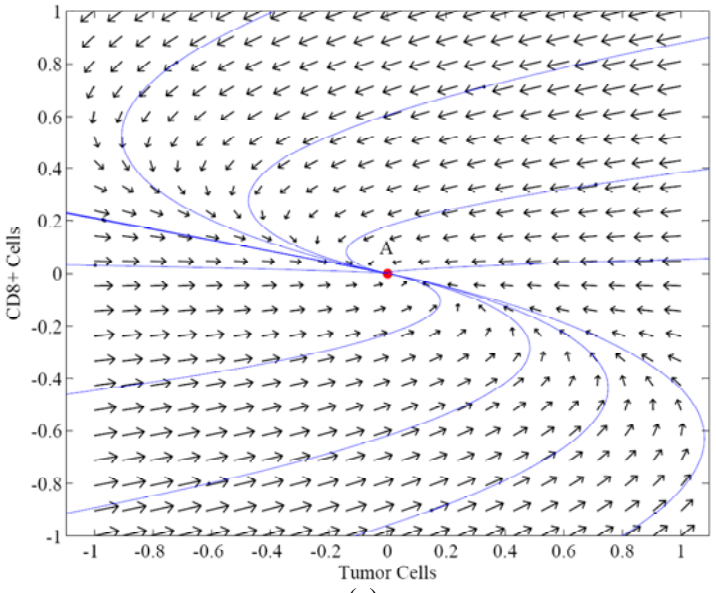

(a)

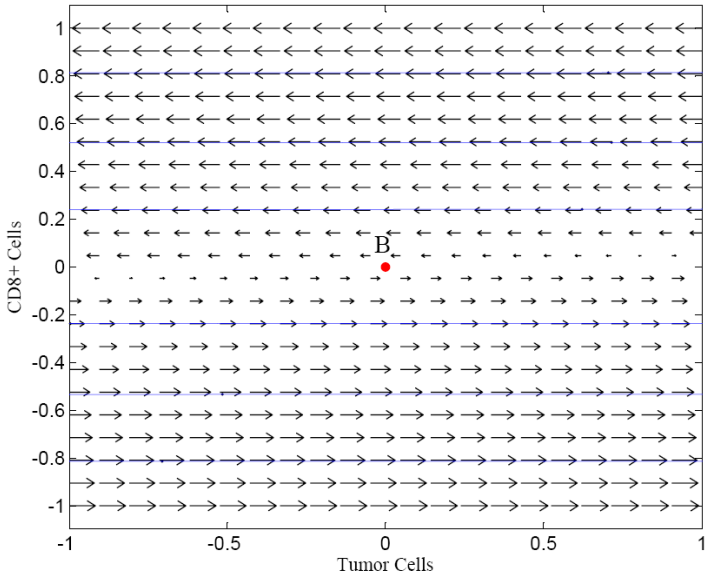

(b)

Figure 3. Linearization of the system about the equilibrium points *A* and *B*

For the case T=0 (healthy state), assume that no tumor is present [$T(0) = 0$]. Thus

$$\frac{dT}{dt} = 0, \qquad \frac{dN}{dt} = \sigma - fN, \qquad \frac{dL}{dt} = -mL.$$

Hence, $N(t) \to \frac{\upsilon\sigma}{f}$ and $N(t) \to 0$, as $t \to \infty$. This shows that, without a tumor, the system converges to a stable state [14].

Since the system (1)-(3) is highly nonlinear, the stability of the system may also be found through examining an appropriate Lyapunov function [11]:

$$V(x) = \frac{1}{2}L^2 + \frac{1}{2}N^2 + \ln(T+1). \tag{7}$$

3.2. Lyapunov Stability

If, in a ball B_r there exists a scalar function V of the state x, with continuous first order derivatives, such that

- $V(x)$ is positive definite,
- $\dot{V}(x)$ is negative definite,
- $V(x) \to \infty,\ as\ \ x \to \infty,$

then the equilibrium at the origin is locally stable [11].

Define a Lyapunov function as (7), which is clearly positive definite. Along the trajectories of the system, we have

$$\dot{V}(x) = L\dot{L} + NN^{\cdot} + \frac{\dot{T}}{1+T}.$$

so,

$$\dot{V}(x) = L\left[-mL + \frac{jD^2}{k+D^2}L - qLT + rNT\right] + N\left[\sigma - fN + \frac{gT^2}{h+T^2}N - pNT\right] + \frac{[aT(1-bT) - cNT - D]}{1+T}.$$

By plotting the surface and contour graphs of $Z(T, L, V(x))$ (Fig. 4), we can see that one equilibrium point is Lyapunov unstable ($\dot{V}(x) > 0$) and two equilibrium points are Lyapunov stable ($\dot{V}(x) < 0$). Therefore, Lyapunov stability of the system is in agreement with those illustrated in Section 3.1.

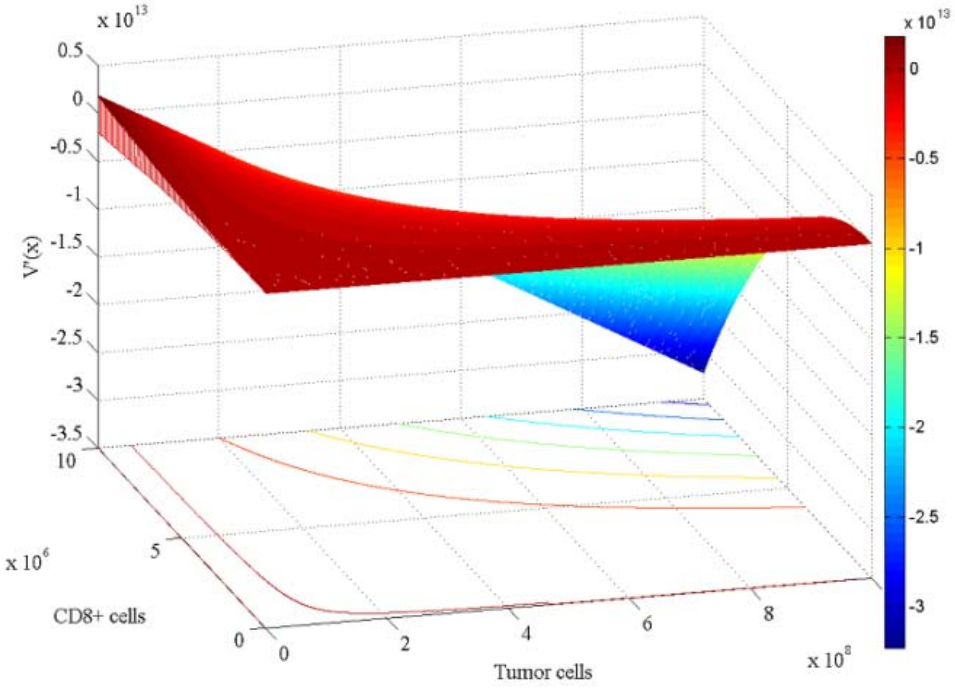

(a)

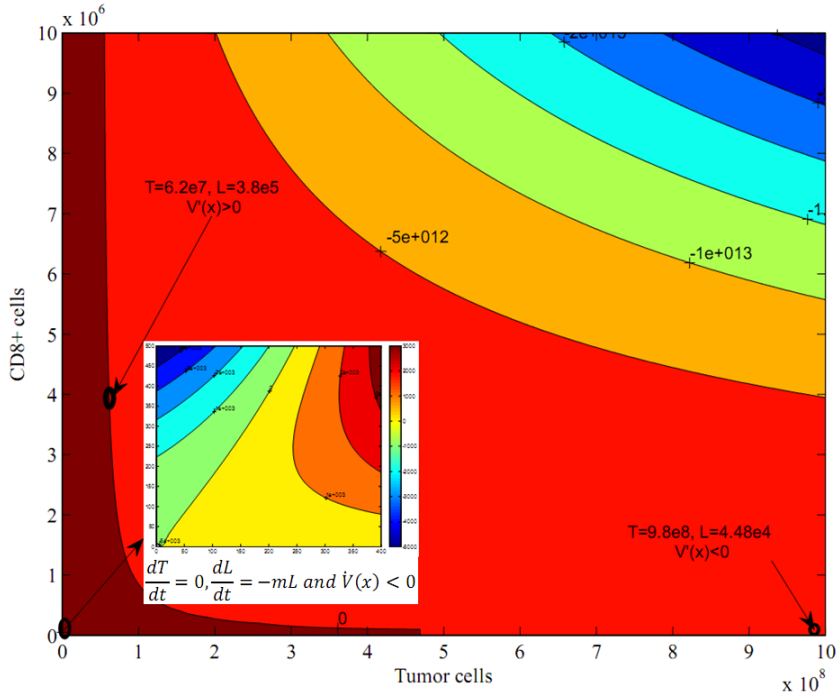

(b)

Figure 4. (a) surface and (b) contour graphs of proposed Lyapunov functions

Overall, the parameter set we are working with lies in a region where we have two stable states: one with a large tumor burden, and one with a zero tumor burden. Our goal is to drive the system toward the zero tumor burden point.

We test two separate cases, with and without the vaccine therapy (Fig. 5 (a) and 5 (b)), both of which place us initially in the basin of attraction of the large tumor burden equilibrium point. From Fig. 4, we see that when the system progresses naturally without any vaccine intervention, the tumor burden overwhelms the system, and so the patient will not survive. The second approach employs immunotherapy in the form of an injection of 1.2×10^7 highly activated $CD8^+$T cells from day 7 (Fig. 5 (b). This $CD8^+$ T cells injection is meant to represent the Tumor Infiltrating Lymphocyte (TIL) treatments used for certain patients [9]. For an initial tumor challenge of 1×10^7 cells, the tumor survives despite the vaccine intervention.

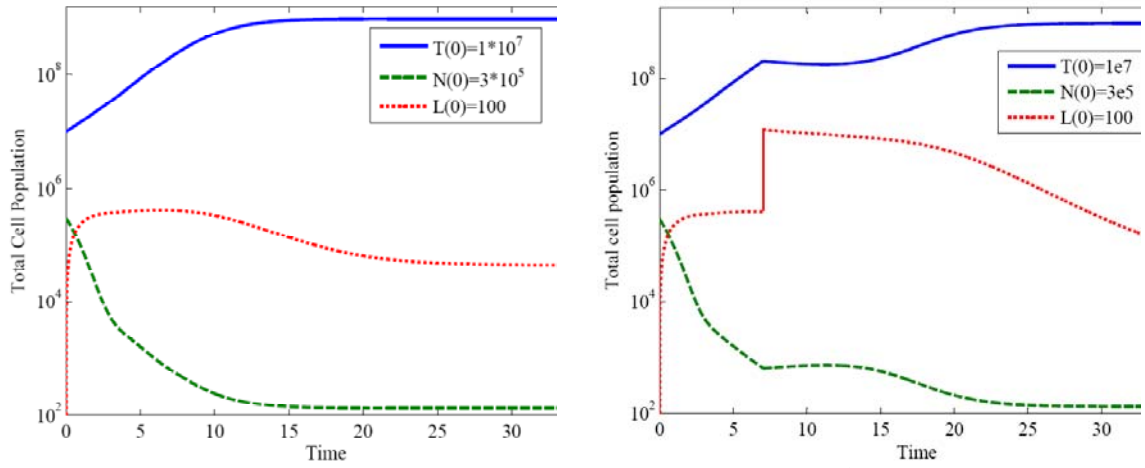

(a) (b)

Figure 5. (a) behavior of the system of equations in absence of vaccine (b) behavior of the system of equations in presence of vaccine

4. Quadratic Control

The optimal treatment approach employs immunotherapy in the form of an injection of highly activated $CD8^+$T cells. For the model described by (1)-(3), we now use the control *u(t)* to decrease the tumor burden while minimizing total vaccine injection. We add the control term to the system of differential equations.

The system with the vaccine injection is then given by

$$\frac{dT}{dt} = aT(1-bT) - cNT - D \tag{8}$$

$$\frac{dN}{dt} = \sigma - fN + \frac{gT^2}{h+T^2}N - pNT \tag{9}$$

$$\frac{dL}{dt} = -mL + \frac{jD^2}{k+D^2}L - qLT + rNT + u(t) \tag{10}$$

$$D = d\frac{(L/T)^{\lambda}}{s+(L/T)^{\lambda}}T. \tag{11}$$

We first analyze the theoretically more tractable quadratic control in order to present a clear picture of the process.

We minimize the objective functional

$$J(u) = \int_0^{t_f}\left(-\mathrm{L} + \mathrm{T} - \mathrm{N} + \left(\frac{1}{2}\right)\mathrm{wu}^2\right)\mathrm{dt}, \tag{12}$$

which is a quadratic form with respect to the control *u*, subject to (8)-(11). First, we prove that there exists an optimal control that minimizes the objective functional (12).

4.1. Necessary Conditions for Optimality

Theorem 2 (Existence). Given the objective functional $J(u) = \int_0^{t_f}(-L + T - N + \left(\frac{1}{2}\right)wu^2)dt$, where $U = \{u(t)\ \text{piecewise continuous}|0 \le u(t) \le 1 \quad \forall t \in [0, t_f]\}$ subject to system (8)-(11) with $T(0) = T_0$, $N(0) = N_0$, $L(0) = L_0$, there exists an optimal control u^* such that $\min_{\mathrm{u(t)}\in[0,1]} J(u) = J(u^*)$, if the following conditions are met:

1. The class of all initial conditions with a control $u(t)$ in the admissible control set along with each state equation being satisfied is not empty.

2. The admissible control set *U* is closed and convex.

3. Each right hand side of the state system is continuous, bounded above by a sum of the bounded control and the state, and can be written as a linear function of u with coefficients depending on time and state.

4. The integrand of $J(u)$ is convex on *U* and bounded below by $-\mathrm{c}_2 + \mathrm{c}_3|\mathrm{u(t)}|^2$, with $c_3 > 0$.

Proof. The first step is to prove that given an admissible control, the state equations have bounded solutions. In proving this, a standard existence theory of first-order nonlinear differential equation, wherein they bound the upper value of the state is given by a function of initial state and final time. It should be noted here that optimal control solutions have already been found for all these problems in different papers [5, 8]. So, it is worthwhile to refer to those solutions.

For proving the existence of an optimal control for the state system, the set of conditions 1 through 4 have to be satisfied. Since the boundedness of the solution (for admissible control) has already been established and the set of controls $u(t) \in U$ is closed and convex (by definition), two of these conditions are automatically satisfied.

For the third condition, the system is bilinear in the control and can be rewritten as

$$\vec{f}(t, \vec{X}, u) = \vec{\alpha}(t, \vec{X}) + \begin{pmatrix} 0 \\ 0 \\ u \end{pmatrix},$$

where $\vec{X} = \begin{pmatrix} T \\ N \\ L \end{pmatrix}$ and $\vec{\alpha}$ is a vector valued function of $\vec{X}$. Using that the solutions are bounded, we see that

$$|\vec{f}(t,\vec{X},u)| \leq \left|\begin{pmatrix} a & 0 & 0 \\ 0 & g & 0 \\ 0 & 0 & j \end{pmatrix}\begin{pmatrix} T \\ N \\ L \end{pmatrix}\right| + \left|\begin{pmatrix} 0 \\ \sigma \\ rag+u \end{pmatrix}\right| \leq c_1(|\vec{X}|+u),$$

Where c_1 depends on the coefficients of the system.

For the fourth condition, we need to show

$$J(t,T,N,L,(1-e)u_1+eu_2) \leq (1-e)J(t,T,N,L,u_1)+eJ(t,T,N,L,u_2).$$

We analyze the difference of $J(t,T,N,L,(1-e)u_1+eu_2)$ and $(1-e)J(t,T,N,L,u_1)$

$+eJ(t,T,N,L,u_2)$ to see that

$J(t,T,N,L,(1-e)u_1+pu_2)-[(1-e)J(t,T,N,L,u_1)+eJ(t,T,N,L,u_2)] = \frac{\omega}{2}(e^2-e)(u_1-u_2)^2$.

Since, $e \in (0,1)$ implies $(e^2-e)<0$ and $(u_1-u_2)^2>0$,

the expression $\frac{\omega}{2}(e^2-e)(u_1-u_2)^2<0$ this implies that

$$J(t,T,N,L,(1-e)u_1+pu_2) \leq (1-e)J(t,T,N,L,u_1)+eJ(t,T,N,L,u_2).$$

Lastly,

$$-L(t)+T(t)-N(t)+\left(\frac{w}{2}\right)(u(t))^2 \geq -L(t)-N(t)+\left(\frac{w}{2}\right)(u(t))^2 \geq -c_2+c_3|u(t)|^2.$$

With the existence of the quadratic optimal control established, we now characterize the optimal control using the Pontryagin's Maximum Principle. In the next theorem, we use $\frac{d\lambda_i}{dt}=\dot{\lambda_i}(t)$.

Theorem 3. (Characterization). Given an optimal control u^* and solutions to the corresponding state system that minimizes the functional $J(u)=\int_0^{t_f}\left(-L+T-N+\left(\frac{1}{2}\right)wu^2\right)dt$ subject to condition (8)-(11), there exist adjoint variables λ_i for $i = 1, 2, 3$, satisfying

$$-\frac{\partial H}{\partial T}=\dot{\lambda_1}=-1+\lambda_1(-a+2abT+cN+\alpha_1)+\lambda_2\left(-\frac{hN}{(h+T^2)^2}+pN\right)+\lambda_3\left(-\frac{j\alpha_3 kL}{(k+D^2)^2}+qL-rN\right)$$

$$\frac{-\partial H}{\partial N}=\dot{\lambda_2}=1+\lambda_1(cT)+\lambda_2\left(f-\frac{gT^2}{h+T^2}+pT\right)+\lambda_3(-rT)$$

$$\frac{-\partial H}{\partial L}=\dot{\lambda_3}=1+\lambda_1(\alpha_2)+\lambda_3(m-\frac{j\alpha_4 kL}{(k+D^2)^2}-\frac{jD^2}{k+D^2}+qT)$$

$$\alpha_1=-\frac{dT\lambda s\left(\frac{L}{T}\right)^{\lambda-1}\left(\frac{L}{T^2}\right)}{\left(s+\left(\frac{L}{T}\right)^{\lambda}\right)^2}+\frac{d\left(\frac{L}{T}\right)^{\lambda}}{s+\left(\frac{L}{T}\right)^{\lambda}}$$

$$\alpha_2 = \frac{dT\lambda s\left(\frac{L}{T}\right)^{\lambda-1}\left(\frac{1}{T}\right)}{\left(s+\left(\frac{L}{T}\right)^{\lambda}\right)^2}$$

$$\alpha_3 = \frac{(d^2T^2)\left[s^2 2\lambda \ \ ^{2\lambda-1}\left(-\frac{L}{T^2}\right) + 2s\lambda\left(\frac{L}{T}\right)^{3\lambda-1}\left(-\frac{L}{T^2}\right)\right]}{\left(s+\left(\frac{L}{T}\right)^{\lambda}\right)^4} + \frac{2d^2T\left(\frac{L}{T}\right)^{2\lambda}}{\left(s+\left(\frac{L}{T}\right)^{\lambda}\right)^2}$$

$$\alpha_4 = (d^2T^2)\frac{\left[s^2 2\lambda\left(\frac{L}{T}\right)^{2\lambda-1}\left(\frac{1}{T}\right) + 2s\lambda\left(\frac{L}{T}\right)^{3\lambda-1}\left(\frac{1}{T}\right)\right]}{\left(s+\left(\frac{L}{T}\right)^{\lambda}\right)^4},$$

A where $\lambda_i(t_f) = 0$, for i = 1, 2, 3. Moreover, $u^*(\mathrm{t})$ can be represented by

$$u^*(\mathrm{t}) = \min\left(1, \left(-\frac{\lambda_3}{\mathrm{w}}\right)^+\right),$$

where,

$$r^+ = \begin{cases} r, & r \geq 0 \\ 0, & r < 0. \end{cases}$$

Proof. For this functional, the Hamiltonian is given by

$$H = -L + T - N + \left(\frac{1}{2}\right)wu^2 + \lambda_1(aT(1-bT) - cNT - D) + \lambda_2\left(\sigma - fN + \frac{gT^2N}{h+T^2} - pNT\right) + \lambda_3\left(-mL + \frac{jD^2L}{k+D^2} - qLT + rNT + u\right). \quad (10)$$

Since the control is bounded, we form the Lagrangian as follows:

$$\mathcal{L} = H + w_1(t)u(t) - w_2(t)\big(1-u(t)\big).$$

Here, H is the Hamiltonian as defined in (10) and $w_{\mathrm{i}}(\mathrm{t}) \geq 0$ are penalty multipliers such that $w_1(t)u(t) = 0$ and $w_2(t)\big(1-u(t)\big) = 0$ at the optimal control u^*.

To characterize u^*, we analyze the necessary optimality condition $\frac{\partial \mathcal{L}}{\partial u} = 0$. Here, $\frac{\partial \mathcal{L}}{\partial u} = \frac{\partial H}{\partial u}$

$$-w_1 + w_2 = wu + \lambda_3 - w_1 + w_2 = 0.$$

Using standard optimality arguments, we characterize the optimal control for $u(t)$ as

$$u^*(t) = \min\left(1, \left(-\frac{\lambda_3}{w}\right)^+\right).$$

We also note that the second derivative of the Lagrangian with respect to u is positive, and so a minimum occurs at u^*.

5. Numerical Simulations for Quadratic Control

The problem of numerical integration of the tumor system with vaccine can now be considered as a two boundary value problem for which the initial states of the control variables are known and the final states of the co-state variables are known. Here, we present the numerical solution of the controlled nonlinear tumor system with vaccine to explore the possibility of the optimal control of this system. a numerical solution of the controlled tumor system is displayed in Figures 6(a)-(d). One can see that the largest dose of vaccine is administered at the beginning of the time period, and then is lowered to a small but non-zero and very slowly decreasing level for the remainder of the treatment period. The tumor is driven to near-zero, while the population of immune cells is rising.

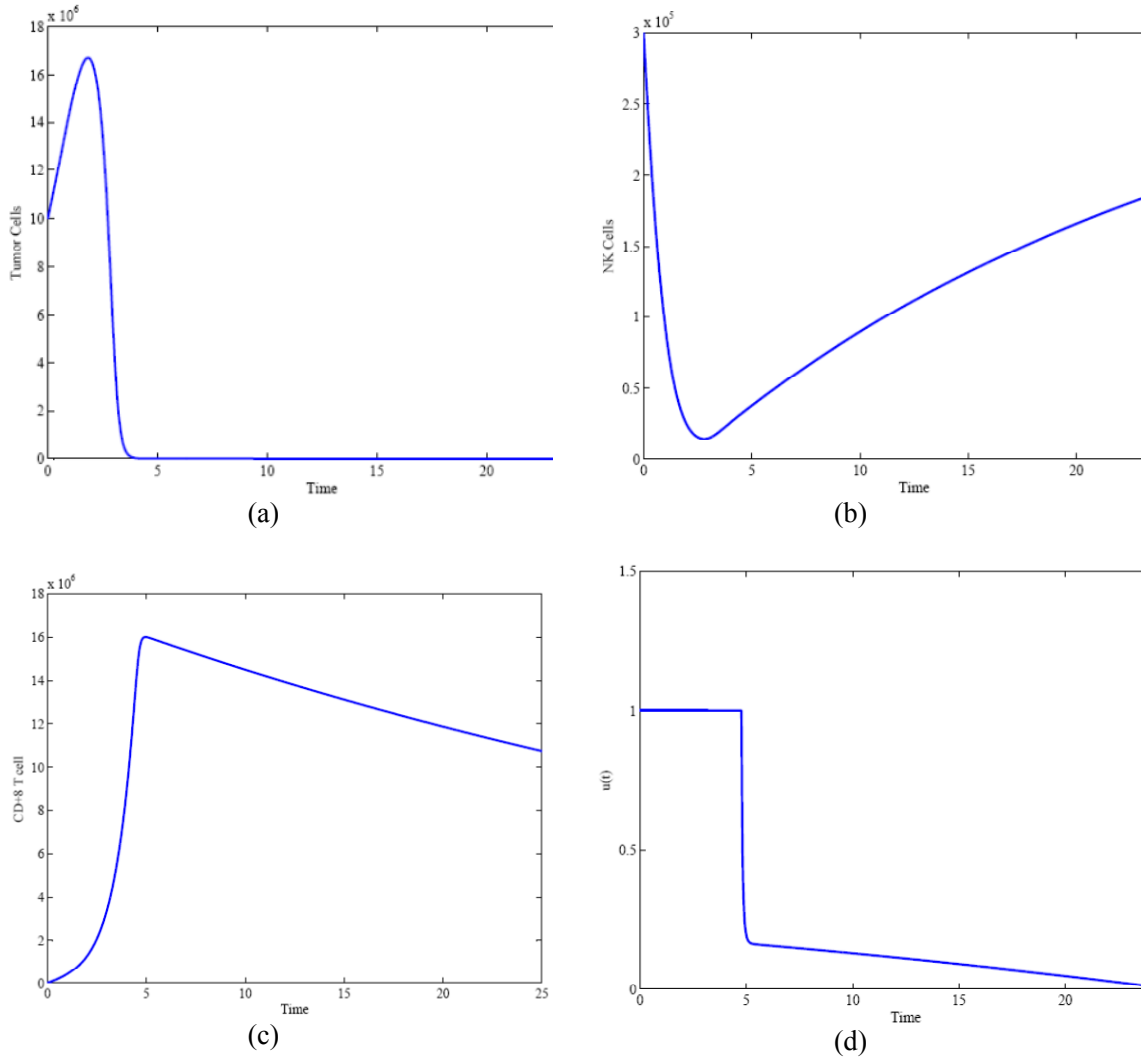

Figure 6. Quadratic control situations: $T(0) = 1\times10^7$ cell, $N(0) = 3\times10^5$ and $L(0) = 100$

Therefore, this is where the optimal control proves to be of some use. The protocol suggested by the optimal control algorithm dictates that the vaccine be administered continuously over relatively long periods of time-on the order of days. Fig. 6 shows the evolution of the system with the optimal control treatment administered. Optimal control therapy is superior to traditional pulsed therapy in the sense that the tumor burden is driven to low levels, and the NK cell population stays at higher levels for longer periods of time. For the weaker immune system, traditional therapy fails to bring the system into the desirable basin of attraction at all (see Fig. 5 (b)), whereas the optimal control protocol does successfully pushs the system into the zero tumor burden basin of attraction. Therefore, the medicine eventually can be shut off, and the tumor continues to diminish to zero without further intervention.

6. Conclusion

We characterized the ODE system dynamics by locating equilibrium points and determining stability properties. By applying optimal control theory, we seeked to minimize the cost function associated with the vaccine therapy looking for at minimization of the tumor cells. Global existence of a solution was shown for the model and existence of an optimal control was proven. An analysis and a numerical integration example for the controlled system were carried out. The protocol suggested by the optimal control algorithm dictates that the vaccine be administered continuously over relatively long periods of time, on the order of days.

Acknowledgements

We are grateful to reviewers for their helpful and useful comments and suggestions.

References

[1] Burden, T., Ernstberger, J. and Renee, F. K. (2004), Optimal control applied to immunotherapy ,*Discrete and Continuous Dynamical Systems*, Series B., 4, 135-146.

[2] Castiglione, F. and Piccoli, B. (2007), Cancer immunotherapy, mathematical modeling and optimal control, *Journal of Theoretical Biology*, 247, 723-732.

[3] Castiglione, F. and Piccoli, B. (2006), Optimal control in a model of dendritic cell transfection immunotherapy, *Bullten of Mathematical*,*Biology* 68, 255-274.

[4] Chamberlain, R. S. (1999), Prospects for the therapeutic use of anticancer vaccines, Drugs, 309-325.

[5] De Pillis, L. G., Gu W., Fister K.R., Head T., Maples K., Murugan A., Neal T. and Yoshida K. (2007), Chemotherapy for tumors: an analysis of the dynamics and a study of quadratic and linear optimal controls, *Mathematical Biosciences*, 209, 292-315.

[6] De Pillis, L. G., Gu W. and Radunskaya A.E. (2006), Mixed immunotherapy and chemotherapy of tumors: modeling, applications and biological interpretations, *Journal of Theoretical Biology*, 238, 841-862.

[7] De Pillis, L. G, Radunskaya A. E. and Wiseman Ch. L.)2005(, A validated mathematical model of cell-mediated immune response to tumor growth, *Cancer Research*, 65, 7950-7958.

[8] De Pillis, L. G., Gu W. and Radunskaya A.E. (2003), The dynamics of an optimally controlled tumor model: a case study, *Mathematical and Computer Modeling*, 37, 1221-1244.

[9] Dudley, M.E. , Wunderlich J.R., Robbins P.F., Yang J.C., Hwu P., Schwartzentruber D.J., Topalian S.L., Sherry R., Restifo N.P., Hubicki, A.M., Robinson M.R., Raffeld M., Duray P., Seipp, C.A., Rogers-Freezer, L., Morton K.E., Mavroukakis S.A., White D.E. and Rosenberg S.A.)2002(, Cancer regression and autoimmunity in patients after clonal repopulation with antitumor lymphocytes, *Science*, 298, 850-854.

[10] Fister, K.R. and Donnelly, J. H. (2005) ,Immunotherapy: an optimal control theory approach, *Mathematical Biosciences and Engineering*, 2, 499-510.

[11] Ghaffari, A. and Nasserifar, N. (2009), Mathematical modeling and lyapunov-based drug administration in cancer chemotherapy, *Iranian Journal of Electrical & Electronic Engineering*, 3, 151-158.

[12] Gilboa, Nair, S.K. and Lyerly, H.K. (1998), Immunotherapy of cancer with dendritic-cell-based vaccines, *Cancer Immunology Immunotherapy,* 46, 82-87.

[13] Greten, T.F. and Jaffee E.M. (1999), Cancer vaccines, *Journal of Clinical Oncology*, 17, 1047-1060.

[14] Gowal, V., De Giacomi, M. and Le Boudec, J.Y. (2007), Comment on: a validated mathematical model of cell-mediated immune response to tumor growth, *Cancer Research*, 67, 8419-8421.

[15] Kirschner, D. and Panetta, J.C. (1998), Modeling immunotherapy of tumor immune interaction, *Journal Mathematical Biology*, 37, 235-252.

[16] Michael, C. and Perry, M. (2001), The Chemotherapy Source Book, 3rd Edition, Lippincott Williams & Wilkins Publishers.

[17] Piccoli, B. and Castiglione, F. (2006), Optimal vaccine scheduling in cancer immunotherapy, *Physica*, A., 370, 672-680.